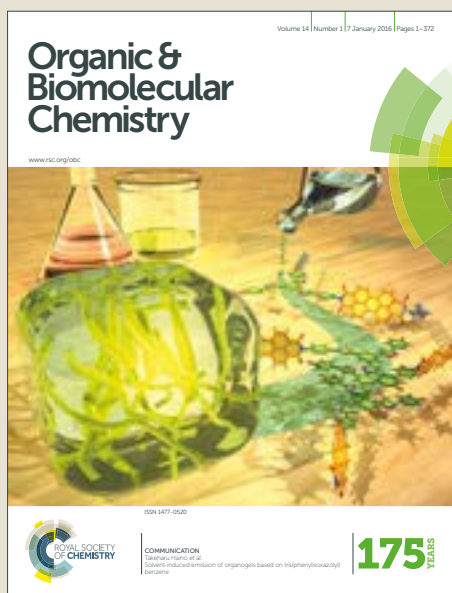


# Organic & Biomolecular Chemistry

Accepted Manuscript



This article can be cited before page numbers have been issued, to do this please use: J. Wang, X. Hu, D. Wang, C. Xie, W. Lu, J. Song, R. Wang, C. Gao and M. Liu, *Org. Biomol. Chem.*, 2018, DOI: 10.1039/C8OB00953H.



This is an Accepted Manuscript, which has been through the Royal Society of Chemistry peer review process and has been accepted for publication.

Accepted Manuscripts are published online shortly after acceptance, before technical editing, formatting and proof reading. Using this free service, authors can make their results available to the community, in citable form, before we publish the edited article. We will replace this Accepted Manuscript with the edited and formatted Advance Article as soon as it is available.

You can find more information about Accepted Manuscripts in the [author guidelines](#).

Please note that technical editing may introduce minor changes to the text and/or graphics, which may alter content. The journal's standard [Terms & Conditions](#) and the ethical guidelines, outlined in our [author and reviewer resource centre](#), still apply. In no event shall the Royal Society of Chemistry be held responsible for any errors or omissions in this Accepted Manuscript or any consequences arising from the use of any information it contains.



Journal Name

ARTICLE

## 2-Aminoimidazole facilitates efficient gene delivery in low molecular weight poly(amidoamine) dendrimer

Jing Wang,<sup>a</sup> Xuefeng Hu,<sup>a</sup> Dongli Wang,<sup>a</sup> Cao Xie,<sup>a</sup> Weiyue Lu,<sup>a</sup> Jie Song,<sup>a</sup> Ruifeng Wang,<sup>a</sup> Chunli Gao,<sup>b</sup> and Min Liu\*<sup>a</sup>

Received 00th January 20xx,  
Accepted 00th January 20xx

DOI: 10.1039/x0xx00000x

www.rsc.org/

Functional groups have shown great potential in gene delivery. However a number of the reported functional groups can only overcome one certain physiological barrier, resulting in limited transfection efficiencies. Based on the structure-activity relationships of both imidazolyl and guanidyl, we designed a novel multifunctional group, 2-aminoimidazole (AM), for gene delivery. Modifying with AM group, the transfection efficiency of low molecular weight poly(amidoamine) (G2) was 200 times greater than the parent dendrimer in vitro. In contrast, the transfection efficiency of G2 showed a trend of decrease when it grafted with imidazole. Assays revealed that AM group played multiple roles in gene delivery, including condensing DNA into monodisperse nanoparticles of 80–90 nm in diameter, achieving nearly ten times higher cellular-uptake efficacy, enhancing abilities of endosome/lysosome escape and nuclear localization. What's more, AM showed low toxicity. These results demonstrate that AM group could be a promising tool in non-viral gene delivery.

### Introduction

Non-viral vectors have attracted increasing attention due to their low immunogenicity, flexible DNA loading capacity and tailorable properties.<sup>1–5</sup> However, their applications are limited by low transfection efficiency.<sup>6,7</sup> Non-viral vectors need to overcome the following physiological barriers to achieve DNA delivery: (1) potential degradation by endonucleases and phagocytosis by the reticuloendothelial system in the blood, (2) cellular internalization across the amphipathic cytomembrane with negatively charged regions, (3) degradation by lysosomal enzymes and transportation into the nucleus.<sup>8–10</sup> Each of these physiological barriers has the potential to significantly reduce the transfection efficiency of non-viral DNA delivery.

These barriers might be overcome owing to the developments in material sciences, which have yielded new functional groups as gene delivery enhancer, such as hydrophobic molecules, targeting molecules, cell penetrating peptides, guanidyl, imidazolyl, fusion proteins and nuclear localization signal peptides.<sup>11–20</sup> These functional groups aim to enhance DNA condensation, cellular uptake, endosome/lysosome escape and nuclear localization. Of the

functional groups listed, we are particularly interested in imidazolyl and guanidyl. Derived from histidine, imidazolyl can facilitate the endosomal escape of DNA complexes via a “proton sponge” mechanism, due to its high buffering capacity at endosomal pH. Guanidyl, from arginine, can be beneficial not only to DNA condensation, but also membrane transportation, due to forming bidentate hydrogen bonds with phosphate groups both in the DNA and the cell membrane.<sup>21</sup> Based on the structure-activity relationships of both imidazolyl and guanidyl, we predicted that integrating imidazolyl and guanidyl into one functional group could produce a cumulative effect. Therefore, we designed a novel multifunctional group, 2-aminoimidazole (AM), for DNA delivery, which contains an amino group at position 2 of the imidazole ring. It was reported that the pKa of AM was 8.46, which was about 1.5 units higher than imidazole (7.01) and 5 units lower than guanidine (13.4).<sup>22,23</sup> We speculated that AM group would increase DNA condensation, cytomembrane penetration, endosome/lysosome escape and nuclear localization concurrently. To verify this hypothesis, we grafted PAMAM generation 2 (G2) with AM to develop a cationic polymer (G2-AM) as a non-viral vector. G2 was chosen as the basis for modification with AM for the following reasons: first, G2 has a well-defined number of amine groups on the surface, and is easy to be chemically modified; second, G2 is relatively well tolerated; third, G2 has a poor transfection efficiency due to its low density of primary and tertiary amine groups, making it easier to assess improvements in performance resulting from AM modification. Interestingly, AM modification significantly enhanced the transfection efficiency of G2 without introducing additional toxicity. G2-AM was found to have a transfection efficiency ~200 times greater than that of G2 alone in vitro,

<sup>a</sup> Department of Pharmaceutics, School of Pharmacy Fudan University & Key Laboratory of Smart Drug Delivery (Fudan University), Ministry of Education Shanghai, 201203 (P.R. China)

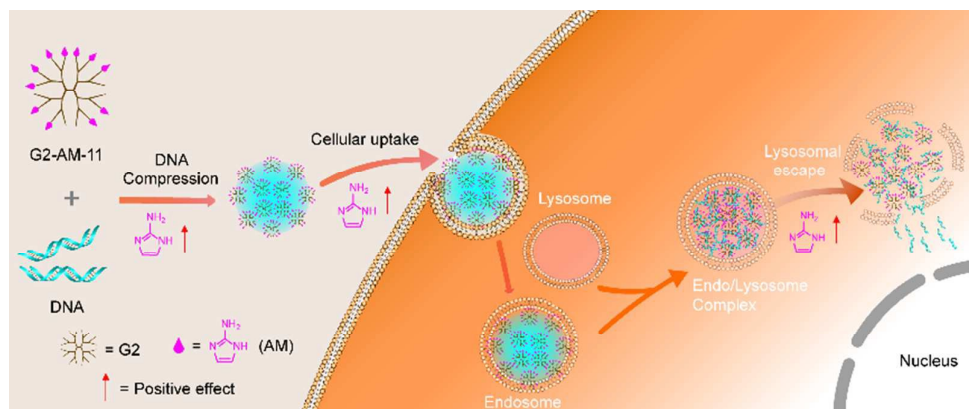
<sup>b</sup> Department of Otolaryngology-Head and Neck Surgery, Eye and ENT Hospital Fudan University

† Footnotes relating to the title and/or authors should appear here.

Electronic Supplementary Information (ESI) available: [details of any supplementary information available should be included here]. See DOI: 10.1039/x0xx00000x

and was more efficient than Lipofectamine 2000. Imidazolyl-modified G2 (G2-M) was also synthesized as a control, and showed no significant improvement compared with the parent dendrimer. Finally, we investigated the transfection mechanism of G2-AM as a gene vector, including DNA

packaging, buffering capacity, cell uptake and nuclear localization. The data showed that AM could contribute to overcoming the multiple physiological barriers that non-viral vectors encounter. Our results demonstrate that the AM group could have potential applications in non-viral gene delivery.



Scheme 1. Effects of AM in efficient gene delivery.

## Results and discussion

### Design and Synthesis of the materials.

We synthesized G2-AM through the reaction of G2 and tert-butyl (4-formyl-1H-imidazol-2-yl) carbamate. The modification ratio of AM was verified by  $^1\text{H}$  NMR spectrum (Figure S4-S7). The resulting materials were termed G2-AM-2, G2-AM-5, G2-AM-8 and G2-AM-11 respectively. As controls, a series of G2 modified with M were obtained (Figure S8-S10), which termed G2-M-3, G2-M-7 and G2-M-11 respectively. Transfection efficiency of above dendrimers were evaluated in HEK293T cells using an enhanced green fluorescent protein (EGFP) plasmid. As shown in Figure S11, G2-AM-11 performed best in HEK293T cells. Therefore, G2-AM-11 was investigated in detail in further studies.

### AM modification condenses DNA into smaller nanoparticles.

Nanoparticle size is a key parameter affecting the cellular uptake efficiency. In general, particles in the 40–200 nm range exhibit cellular uptake *in vitro*.<sup>24</sup> Fig. 2a and 2b show that the G2-AM-11/pGL<sub>3</sub> complex assembled into spherical nanostructures of 80–90 nm in diameter in water at the mass ratio of 12. The control complexes, G2-M-11/pGL<sub>3</sub> and G2/pGL<sub>3</sub>, assembled into irregular shaped nanostructures of 400–1500 nm in diameter, which appeared aggregated. Gel retardation assays were performed to verify whether G2-AM-11 could condense DNA, with G2 and G2-M-11 used as controls. The mass ratios of G2-AM-11 and G2 for complete retardation were both  $\sim 4$ , whereas that of G2-M-11 was  $\sim 8$  (Fig. 2c). Since G2-AM-11 could condense DNA into smaller nanostructures than G2 and G2-M-11, we speculate that there might be other interactions such as hydrogen bonding between G2-AM-11 and DNA.

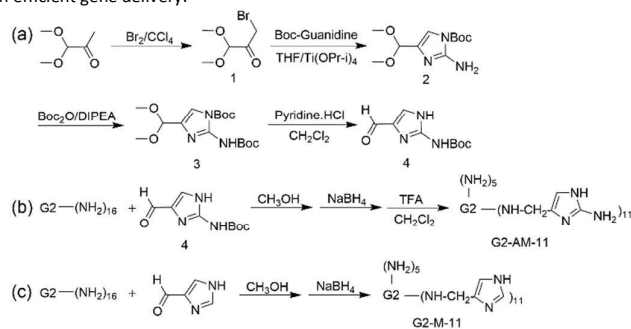


Fig. 1 Synthesis of compound 4 (a), G2-AM-11 (b) and G2-M-11 (c)

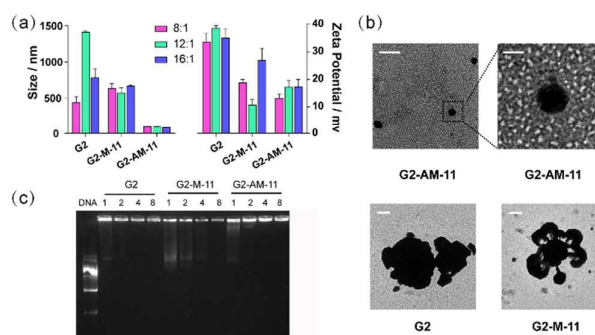


Fig. 2 Formation and characterization of the complexes prepared from G2, G2-M-11, G2-AM-11 and free DNA. (a) Size and zeta potential of the nanoparticles ( $n=3$ ). (b) TEM images of the complexes, with fixed weight ratio of polymer/pGL<sub>3</sub> of 12:1. The scale bar in the top right image is 100 nm, all others are 200 nm. (c) Gel retardation assay of three complexes, using free pGL<sub>3</sub> as a negative control (far left), the number shows the mass ratio of polymer/pGL<sub>3</sub>.

### AM modification greatly improved transfection efficiency *in vitro* and *in vivo*.

Due to its high sensitivity, the luciferase assay was conducted to quantitatively evaluate the transfection efficiency. Fig. 3a showed that the transfection efficiency of G2-AM-11/pGL3 was ~200 times greater than that of G2/pGL3 and ~10000 times greater than that of G2-M-11/pGL3 at a mass ratio of 12:1. What's more, it even performed better than Lipofectamine 2000. The EGFP assay (Fig. 3a) showed similar results. We also investigated the relationship between modification ratio and transfection efficiency. The EGFP and Luciferase assays (Fig. S11) showed that the transfection efficiency increased with the modification ratios of AM, which revealed that AM played an important role in gene delivery. All of the complexes prepared from G2-M showed low transfection efficiency.

Additionally we investigated whether G2-AM-11 could increase transfection efficiency in HeLa cells. Flow cytometry assay showed that G2-AM-11 had higher transfection efficiency in HeLa cells and performed better than the positive control (Fig. S12). The findings described confirmed that AM modification could improve the transfection efficiency of G2.

It is well understood that cationic polymers with high molecular weight show high transfection efficiency accompanied with high cytotoxicity.<sup>25</sup> To investigate whether AM modification could lead to G2 cytotoxicity, we conducted MTT assay to evaluate the cytotoxicity of the polymers and complexes in HEK 293T cells. As shown in Fig. 2b, all complexes prepared from G2, G2-M-11 and G2-AM-11 showed no significant cytotoxicity, with cell viabilities of more than 90%, even when the mass ratio was as great as 16:1. In contrast, the viability of the cells that were co-incubated with the complexes prepared from Lipofectamine was lower than 80%, and decreased to nearly 30% at higher concentration. MTT assay of the polymers was conducted at the concentrations of 0.5 mg/mL, 1 mg/mL and 2 mg/mL (Fig. S14). The results showed that all G2 derivatives had good compatibility with HEK 293T and HeLa cells.

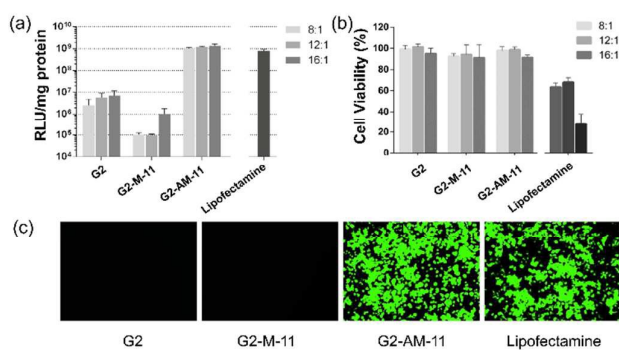


**Fig. 3** In vitro transfection and cytotoxicity studies in HEK 293T cells. (a) Luciferase activities, mass ratios were showed in figure legends, using lipofectamine 2000 as positive controls at the recommended concentration. (b) Cytotoxicity of the complexes, mass ratios were showed in figure legends, compared with lipofectamine 2000. (c) EGFP images, mass ratios were fixed at 12:1.

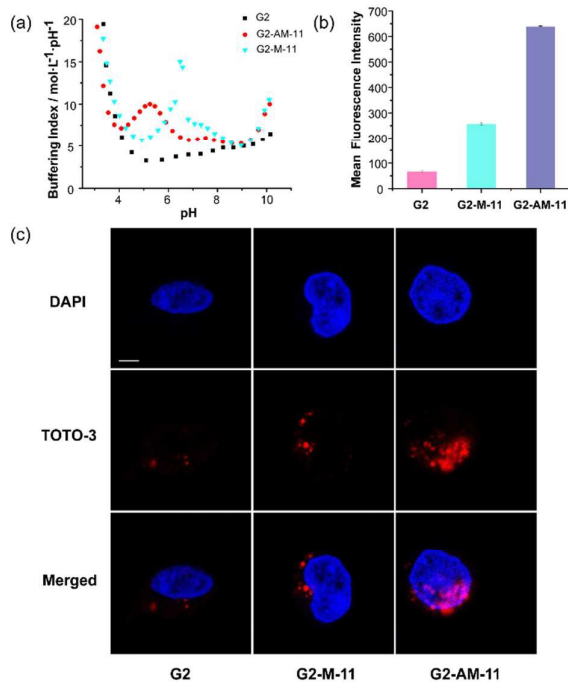


**Fig. 4** Mechanism Assays. (a) Buffering Index ( $\beta$ ) of G2, G2-M-11 and G2-AM-11. (b) Cellular uptake efficiency of the complexes prepared using G2, G2-M-11 and G2-AM-11 in HEK 293T cells. pGL3 plasmid was stained with TOTO-3 and the result is shown as the mean fluorescence of DNA. (c) Cellular uptake images in HEK 293T cells. Cell nuclei were stained with DAPI and pGL3 was stained with TOTO-3. The scale bar is 5  $\mu$ m.

#### Mechanism Studies.

When it comes to the design of non-viral vectors, overcoming only selected obstacles to delivery will not lead to systems capable of improving transfection efficiencies. Due to sophisticated physiological barriers, it appears particularly important to coordinate various functional groups to address more of the challenges presented by the body. Derived from histidine and arginine, imidazolyl and guanidyl have been widely investigated for gene delivery. Joon et al developed imidazolyl and guanidyl grafted G4, and the resulting dendrimers showed significant gene delivery potency.<sup>26a,b</sup> In contrast to that work, we integrated imidazolyl and guanidyl into one functional group, AM, in line with atom economy. Interestingly, a significant distinction between the transfection efficiency of G2-M-11 and G2-AM-11 was observed. To probe the transfection mechanism, we studied the buffering capability and cell uptake of G2-AM-11.

High buffering capacity of non-viral vectors is widely considered as a prerequisite for efficient endosome/lysosome escape. We therefore investigated the buffering capacity of the polymers using acid-base titration.<sup>27-29</sup> To make the results clearer, we adopted buffering index as an indicator of buffering capacity. We compared the buffering index of G2, G2-M-11 and G2-AM-11 in the pH range 2–10. As shown in Fig. 4a, the buffering index of G2 was poorest in the pH range 4–8. This is possibly due to the low density of tertiary amine groups on G2. G2-M-11 and G2-AM-11 performed well across the pH

range. G2-M-11 possessed a higher buffering index in the pH range 5.8–7.0. G2-AM-11 performed better in the pH range 4.2–5.8, with a highest buffering index at pH ~5.2, which was 3 times higher than that of G2. The pH values most frequently found in early endosome, late endosome and lysosome compartments are 6.2–6.3, 5.0–5.5 and 4.5–5.0, respectively.<sup>30–32</sup> Therefore, we speculate that G2-AM-11 might facilitate escape of DNA from both the late endosome and lysosome.

After incubation for 4 h, strong TOTO-3 labeled red fluorescence was present in the cells incubated with G2-AM-11/pGL<sub>3</sub> (Fig. 4c), and it could be observed that the uptake efficiency of G2-AM-11 was nearly 10 times as great as for G2 (Fig. 4b). In addition, there was clear co-localization of TOTO-3 labeled pGL<sub>3</sub> and the nucleus in the cells incubated with the G2-AM-11/pGL<sub>3</sub> complex, which suggests AM modification improved nucleus localization. Most polymers can successfully pass through the cell membrane but fail to reach the nucleus due to the presence of the lysosome and karyotheca. AM modification could overcome these two barriers and ultimately achieve a robust transfection efficiency.

The only difference between M and AM is the additional amino group in the molecular structure of AM. However, M conjugated to G2 had a negative effect on the transfection efficiency. Despite the lower pKa of AM leads to some debate concerning the ability of it to directly mimic a guanidine,<sup>22,33</sup> our results verified AM made some effects similar to guanidyl. The gel retardation assay showed that the minimum mass ratio that could completely condense DNA was larger for G2-M-11 than for G2 and G2-AM-11. TEM images also showed that G2-M-11/pDNA had large particle sizes and irregular shapes, and G2-AM-11 could condense DNA into monodisperse nanoparticles of 80~90 nm in diameter. We speculate that the hydrogen bonding between G2-AM-11 and DNA might result in these differences. Moreover, there are many researches on the enhanced effect of combining hydrogen bonding and cationic elements in gene delivery systems.<sup>34,35</sup> Structure-activity studies showed that the optimal functional groups depends on the parent polymer,<sup>34</sup> which indicated that G2 might not be the best polymer to be modified with AM. We will further investigate more non viral vectors.

## Experimental

### Materials.

Sodium borohydride and boc-guanidine were bought from Sinopharm Chemical Reagent Co. Ltd (Shanghai, China). Imidazole-4-carboxaldehyde and methylglyoxal 1, 1-dimethyl acetal were purchased from J&K Scientific Ltd (Beijing, China). Poly (amidoamine) generation 2 (G2, MW = 3256, 16 NH<sub>2</sub> groups per molecule) was bought from Weihai CY Dendrimer Technology Co. Ltd. (Shandong, China). High molecular weight polyethyleneimine (PEI, branched, MW= 25000) was obtained from Sigma-Aldrich Co. (St. Louis, United States). 4', 6-Diamidino-2-phenylindole (DAPI) was purchased from Dalian Meilun Biology Technology Co. Ltd. (Dalian, China). Lipfectamine 2000 was purchased from Invitrogen (Carlsbad,

United States). TOTO-3 fluorescence dye was bought from Life Technologies (Karlruhe, Germany). Gelred was purchased from Bitoium (Fremont, United States). The Luciferase Assay Kit and the luciferase reporter gene plasmid (pGL3) were products of Promega (Beijing, China). The BCA Protein Assay Kit were purchased from Beyotime (Shanghai, China). The plasmid encoding EGFP (pEGFP-N2) was from Genechem Co. (Shanghai, China).

Human Embryonic Kidney 293T cells (HEK293T cells) was obtained from Shanghai Institute of Cell Biology. Human cervix carcinoma cell lines (HeLa cells) were obtained from the American Type Culture Collection (ATCC). All of the cells lines were maintained in Dulbecco's Modified Eagle Medium (Gibco) supplemented with 10% FBS (Gibco), 100 µg/mL penicillin, and 100 µg/mL streptomycin at 37°C under a humidified atmosphere containing 5% CO<sub>2</sub>.

### Synthesis of G2-AM and G2-M.

To obtain G2-AM, tert-butyl (4-formyl-1H-imidazol-2-yl) carbamate was synthesized by the synthetic route in Figure 1. The detailed steps were as follows.

Synthesis of 3-bromo-1, 1-dimethoxypropan-2-one. Methylglyoxal 1,1-dimethyl acetal (20 g, 0.169 mol) was dissolved in 400 mL CCl<sub>4</sub>, then the solution was cooled to 0°C and Br<sub>2</sub> (32.45 g, 0.202 mol) was added dropwise into the reaction solution. Subsequently, the reaction solution was stirred at room-temperature for 12 h under nitrogen atmosphere. Then, the solution was cooled to 0°C and 100 mL sodium bicarbonate saturated solution was dropped into the system. The organic phase was separated by separating funnel and washed with saturated salt solution for 3 times (3×100mL), dried with anhydrous sodium sulfate. Compound 1 (37.26 g) was obtained by evaporating the organic solvent and directly used for next step without further purification.

Synthesis of tert-butyl 2-amino-4-(dimethoxymethyl)-1H-imidazole-1-carboxylate. Boc-guanidine (10 g, 63 mmol) and compound 1 (18.5 g, 76 mmol) were dissolved in 200 mL tetrahydrofuran, and isopropyl titanate (5.96 g, 21 mmol) was added into the reaction solution. The reaction solution was stirred at room-temperature for 48 h. Subsequently, the crude product was obtained by filtration and evaporating the organic solvent. The crude product was purified by column chromatography (eluent: CH<sub>2</sub>Cl<sub>2</sub>/MeOH/Triethylamine=3/1/0.5) to obtain compound 2 (13.68 g) as a white solid in 84.5% yield. The structure of compound 2 was ascertained by <sup>1</sup>H NMR spectrum (Varian 400 MHz, Palo Alto, USA). (Figure S1)

Synthesis of tert-butyl 2-((tert-butoxycarbonyl) amino)-4-(dimethoxymethyl)-1H-imidazole-1-carboxylate. Compound 2 (5.0 g, 19.45 mmol) was dissolved in 50mL tetrahydrofuran under nitrogen atmosphere. Then N, N-diisopropylethylamine (3.01 g, 23.34 mmol) and di-tert-butyl pyrocarbonate (5.08 g, 23.34 mmol) were added into the flask subsequently and they were stirred at room temperature for 12 h. Then the organic solvent was evaporated under reduced pressure and the mixture was re-dissolved with CH<sub>2</sub>Cl<sub>2</sub>, washed with saturated salt solution and dried with anhydrous sodium sulfate. The

crude product was purified by column chromatography (eluent:  $\text{CH}_2\text{Cl}_2/\text{CH}_3\text{COOCH}_2\text{CH}_3=5/1$ ) to get compound 3 as a white solid (6.42 g) in 92.1% yield. The structure of compound 3 was ascertained by  $^1\text{H}$  NMR spectrum. (Figure S2)

Synthesis of tert-butyl (4-formyl-1H-imidazol-2-yl) carbamate. Compound 3 (2.0 g, 5.6 mmol) was dissolved in 20 mL  $\text{CH}_2\text{Cl}_2$  and the reaction was cooled to  $0^\circ\text{C}$ . Then pyridine hydrochloride was added into the reaction solution and the mixture was stirred at room-temperature overnight. The reaction process was detected by TLC. Following the completion of the reaction, 10 mL water was poured into the solution and the mixture was washed with saturated salt solution for 3 times ( $3 \times 10\text{ mL}$ ). The organic phase was dried with anhydrous sodium sulfate. The crude product was purified by column chromatography (eluent:  $\text{CH}_2\text{Cl}_2/\text{MeOH}=10/1$ ) to get compound 4 as a white solid (0.99 g) in 84.0% yield. The structure of compound 4 was ascertained by  $^1\text{H}$  NMR spectrum. (Figure S3)

Synthesis of G2-AM and G2-M. G2 and compound 4 were dissolved in methanol at different molar ratios and stirred for 24 h under nitrogen atmosphere. Then equimolar amount (compared with compound 4) of sodium borohydride was added and the mixture was stirred at room-temperature overnight. The solvent was evaporated under reduced pressure to get a yellow solid. Then the solid was dissolved in  $\text{CH}_2\text{Cl}_2$  which contained 20% trifluoroacetic acid and the solution was stirred at room-temperature for 8 h. The mixture was purified by dialysis (MWCO 500-1000 Da) against distilled water which contained a little ammonium hydroxide. The solution was then freeze-dried and their modification ratios were ascertained by  $^1\text{H}$  NMR spectrum (Varian 400 MHz, Palo Alto, USA). (Figure S4-S7) To be a control, imidazolyl modified G2 were synthesized by a similar method between G2 and imidazole-4-carboxaldehyde. The synthesis method was the same as G2-AM unless the lack of taking off the protection base. The products were ascertained by  $^1\text{H}$  NMR spectrum. (Figure S8-S10)

#### Formation and characterization of the complex.

To get the complex, different polymers and pGL3 plasmid were dissolved in double distilled water respectively, and equal volume of the polymer and pGL3 solutions were vortexed for 30 s, then incubated for 30 min at room temperature. The final pGL3 concentration of the complex was  $40 \mu\text{g/mL}$ . All of the complexes in this article were prepared in this method unless otherwise noted.

The size distribution and zeta potential of the complexes prepared from different polymers were determined by dynamic light scattering (DLS). The formed complexes were stained by phosphotungstic acid and their morphology structures were characterized using transmission electron microscopy (TEM). To investigate the DNA condensation ability of the polymers, the complexes were prepared and analyzed by 1% agarose gel electrophoresis (120V, 40min).

#### EGFP Assay.

Cells were seeded in a 48-well plate at a density of  $2 \times 10^4$  /well and incubated 24 h before transfection, then the medium was

replaced with 0.5 mL serum-free medium and 0.05 mL complex, and each well included  $2 \mu\text{g}$  pEGFP-N2. The medium was changed to culture medium containing 10% serum after incubation at  $37^\circ\text{C}$  for 4 h. Cells were further incubated for 44 h before determination. Transfection efficiency was determined with an inverted fluorescence microscope (Leica, DMI4000B, Germany) and quantitatively measured by flow cytometry.

#### Luciferase Assay.

Cells were seeded in a 48-well plate at a density of  $2 \times 10^4$  /well and incubated 24 h before transfection, then the medium was replaced with 0.5 mL serum-free medium and 0.05 mL complex, and each well included  $2 \mu\text{g}$  pGL3. The pGL3 encoding luciferase was used as the reporter gene in this assay. The medium was changed to culture medium containing 10% serum after incubation at  $37^\circ\text{C}$  for 4 h. Cells were further incubated for 44 h before determination. The transfection efficiency was determined according to the manufacturer's protocols (Promega). Luciferase activity was determined by an Ultra-Weak Luminescence Analyzer (Chuanghe, China). And the total protein concentration of transfected cell lysate was measured by a BCA protein assay kit following the manufacturer's instructions. Data were expressed as RLU/mg protein (relative light units per milligram cellular protein).

#### Cytotoxicity assay.

The cytotoxicity of complex and polymer were determined by MTT assay. Cells were seeded in a 96-well plate at a density of  $3 \times 10^3$  /well and incubated for 24 h, then the media was replaced with 0.2 mL serum-free medium and 0.02 mL complex, and each well included  $0.8 \mu\text{g}$  pGL3. The medium was changed to culture medium containing 10% serum after incubation at  $37^\circ\text{C}$  4 h. Cells were further incubated for 44 h and  $20 \mu\text{L}$  MTT (5 mg/mL) was added to each well and reacted for 4 h at  $37^\circ\text{C}$ . Then the media in each well was replaced by 0.2 mL DMSO and incubated for 4 h. The absorbance at 490 nm was recorded by a microplate reader (Power Wave XS, Bio-TEK, United States). The relative cell viability (%) of the complexes and materials was calculated by  $A_{\text{sample}}/A_{\text{control}} \times 100\%$ , the control group received the same treatments except adding gene complexes or materials.

#### Cell uptake assay.

Cells were seeded in a 24-well plate at a density of  $1 \times 10^5$  /well and incubated for 24 h, then the media was replaced with 0.5 mL serum-free medium and 0.05 mL complex, and each well included  $2 \mu\text{g}$  TOTO-3 labeled pGL3. Result was analyzed by flow cytometry 4 h later.

To investigate its delivery ability to cell nucleus, cells were incubated with TOTO-3 labeled complex for 4 h, then the cell nucleus was stained with a blue fluorescent dye (DAPI). The fluorescent images were visualized with a laser scanning confocal microscope.

#### Buffering capability.

We study the buffering capacity of G2-AM-11 by acid-base titration, with G2 and G2-M-11 as controls. Each polymer was dissolved in 30 mL double distilled water. All of their

## ARTICLE

## Journal Name

concentration was 0.2 mg/mL. Each solution was adjusted to about pH 10 by 0.1 M NaOH solution and then was titrated by 0.1 M HCl in 20  $\mu$ L increments under vigorous stirring condition at room temperature. The pH was measured by a same pH meter and data were recorded when the numerical reading was stable.

### Conclusions

In summary, we designed a novel multifunctional group, 2-aminoimidazole (AM) for gene delivery. Using poly(amidoamine) generation 2 grafted with AM as a gene vector, the transfection efficiency was  $\sim$ 200 times greater than for the parent dendrimer and performed better than Lipofectamine 2000. Assays revealed that AM could be conducive to condensing DNA into small, monodisperse nanoparticles, enhancing cellular penetration, endosome/lysosome escape and nuclear localization. More importantly, unlike other cationic non-viral vectors with high transfection efficiency, G2-AM has a low toxicity. In general, these studies highlight the effects of the AM group in gene delivery and support further investigation into its applications.

### Conflicts of interest

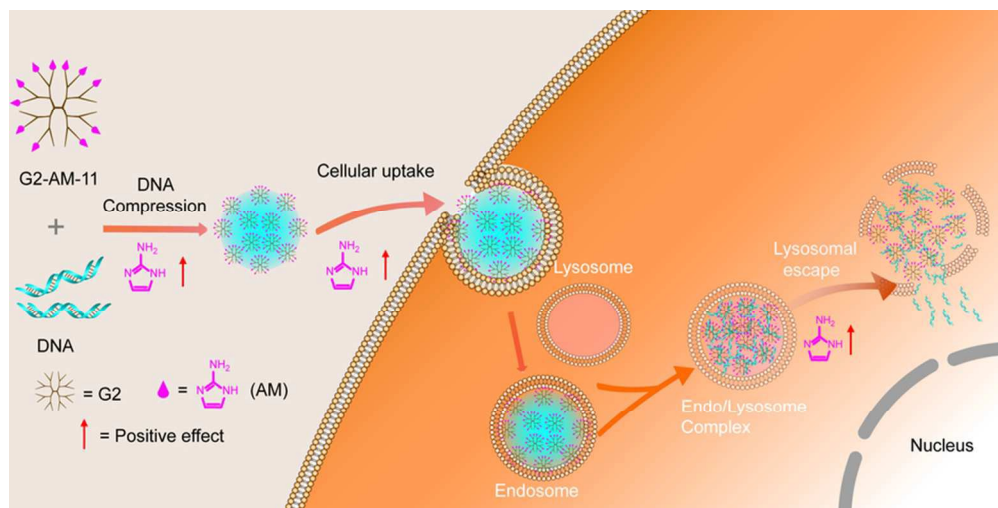
There are no conflicts to declare.

### Acknowledgements

We are grateful for the financial support from the National Science Foundation of China (Grant no. 81473148 and 81690263) and the Foundation Program of Key Laboratory of Smart Drug Delivery of the Ministry of Education.

### Notes and references

- J. Zhou, J. Liu, C. J. Cheng, T. R. Patel, C. E. Weller, J. M. Piepmeier, Z. Jiang, W. M. Saltzman, *Nat. Mater.*, 2011, **11**, 82-90.
- M. Wang, Y. Cheng, *Biomaterials*, 2014, **35**, 6603-6613.
- H. Y. Nam, K. Nam, M. Lee, S. W. Kim, D. A. Bull, *J. Controlled Release*, 2012, **160**, 592-600.
- E. Mastrobattista, S. A. Bravo, M. van der Aa, D. J. Crommelin, *Drug Discov. Today Technol.*, 2005, **2**, 103-109.
- D. Luo, W. M. Saltzman, *Nat Biotechnol.*, 2000, **18**, 33-37.
- F. Liu, L. Huang, *J. Controlled Release*, 2002, **78**, 259-266.
- Z. P. Tolstyka, H. Phillips, M. Cortez, Y. Wu, N. Ingle, J. B. Bell, P. B. Hackett, T. M. Reineke, *ACS Biomater. Sci. Eng.*, 2016, **2**, 43-55.
- M. Morille, C. Passirani, A. Vonarbourg, A. Clavreul, J. P. Benoit, *Biomaterials*, 2008, **29**, 3477-3496.
- M. Ruponen, P. Honkakoski, S. Ronkko, J. Pelkonen, M. Tammi, A. Urtti, *J. Controlled Release*, 2003, **93**, 213-217.
- D. Lechardeur, A. S. Verkman, G. L. Lukacs, *Adv. Drug Deliv. Rev.* 2005, **57**, 755-767.
- M. Li, M. Ehlers, S. Schlesiger, E. Zellermann, S. K. Knauer, C. Schmuck, *Angew Chem. Int. Ed. Engl.*, 2016, **55**, 598-601.
- M. Oba, T. Kato, K. Furukawa, M. Tanaka, *Sci. Rep.*, 2016, **6**, 19913.
- J. E. Dahlman, C. Barnes, O. F. Khan, A. Thiriout, S. Jhunjunwala, T. E. Shaw, Y. Xing, H. B. Sager, G. Sahay, L. Speciner, A. Bader, R. L. Bogorad, H. Yin, T. Racie, Y. Dong, S. Jiang, D. Seedorf, A. Dave, S. K. Singh, M. J. Webber, T. Novobrantseva, V. M. Ruda, A. K. Lytton-Jean, C. G. Levins, B. Kalish, D. K. Mudge, M. Perez, L. Abezgauz, P. Dutta, L. Smith, K. Charisse, M. W. Kieran, K. Fitzgerald, M. Nahrendorf, D. Danino, R. M. Tuder, U. H. von Andrian, A. Akinc, D. Panigrahy, A. Schroeder, V. Koteliensky, R. Langer, D. G. Anderson, *Nat. Nanotechnol.*, 2014, **9**, 648-655.
- M. Wang, H. Liu, L. Li, Y. Cheng, *Nat. Commun.*, 2014, **5**, 3053.
- L. H. Wang, D. C. Wu, H. X. Xu, Y. Z. You, *Angew Chem. Int. Ed. Engl.*, 2016, **55**, 755-759.
- S. Y. Sun, S. Shen, C. F. Xu, H. J. Li, Y. Liu, Z. T. Cao, X. Z. Yang, J. X. Xia, J. Wang, *J. Am. Chem. Soc.*, 2015, **137**, 15217-15224.
- J. L. Choi, J. K. Tan, D. L. Sellers, H. Wei, P. J. Horner, S. H. Pun, *Biomaterials*, 2015, **54**, 87-96.
- T. I. Kim, T. Rothmund, T. Kissel, S. W. Kim, *J. Controlled Release*, 2011, **152**, 110-119.
- Z. Salmasi, W. T. Shier, M. Hashemi, E. Mahdipour, H. Parhiz, K. Abnous, M. Ramezani, *Eur. J. Pharm. Biopharm.*, 2015, **96**, 76-88.
- K. Chen, L. Guo, J. Zhang, Q. Chen, K. Wang, C. Li, W. Li, M. Qiao, X. Zhao, H. Hu, D. Chen, *Acta Biomater.*, 2017, **48**, 215-226.
- E. G. Stanzl, B. M. Trantow, J. R. Vargas, P. A. Wender, *Acc. Chem. Res.*, 2013, **46**, 2944-2954.
- T. S. Bayard, W. S. Walter, L. M. Calvin, *J. Org. Chem.*, 1964, **29**, 3118-3120.
- J. D. Sullivan, R. L. Giles, R. E. Looper, *Curr. Bioactive Comp.*, 2009, **5**, 39-98.
- M. J. Ernsting, M. Murakami, A. Roy, S. D. Li, *J. Controlled Release*, 2013, **172**, 782-794.
- Yang, J.; Zhang, Q.; Chang, H.; Cheng, Y. Surface-Engineered Dendrimers in Gene Delivery. *Chem. Rev.*, 2015, **115**, 5274-5300.
- (a) Y. Bae, E. S. Green, G. Kim, S. J. Song, J. Y. Mun, S. Lee, J. Park, J. Park, K. S. Ko, J. Han, J. S. Choi, *Int. J. of Pharm.*, 2016, **515**, 186-200. (b) L. T. Thuy, S. Mallick, J. S. Choi, *Int. J. Pharm.*, 2015, **492**, 233-43.
- H. Tian, W. Xiong, J. Wei, Y. Wang, X. Chen, X. Jing, Q. Zhu, *Biomaterials*, 2007, **28**, 2899-2907.
- Y. Li, H. Tian, J. Ding, X. Dong, J. Chen, X. Chen, *Polymer Chemistry*, 2014, **5**, 3598-3607.
- Z. Cao, W. Liu, D. Liang, G. Guo, J. Zhang, *Advanced Functional Materials*, 2007, **17**, 246-252.
- F. R. Maxfield, D. J. Yamashiro, *Adv. Exp. Med. Biol.*, 1987, **225**, 189-198.
- S. Ohkuma, B. Poole, *Proc. Natl. Acad. Sci. USA*, 1978, **75**, 3327-3331.
- D. J. Yamashiro, F. R. Maxfield, *J. Cell Biol.*, 1987, **105**, 2713-2721.
- C. Dardonville, I. Rozas, I. Alkorta, *J. Mol. Graphics*, 1998, **16**, 150-156.
- L. Gallego-Yerga, M. Lomazzi, V. Franceschi, F. Sansone, M. C. Ortiz, G. Donofrio, A. Casnati, F. J. Garcia, *Org. Biomol. Chem.*, 2015, **13**, 1708-1723.
- F. Wang, K. Hu, Y. Cheng, *Acta Biomater.*, 2016, **29**, 94-102.



40x20mm (600 x 600 DPI)